

# Comparative Optimization Study of an Isogrid Structure Using Sunflower Optimization and Genetic Algorithm

Francisco, M. B.<sup>1</sup>, Gomes, G. F.<sup>1</sup>, Cunha Jr, S. S.<sup>1</sup>, Da Silva, L. R. R.<sup>1</sup>, Silva, B. A.<sup>2</sup>

<sup>1</sup>Mechanical Engineering Institute, Federal University of Itajubá

1303, Av. BPS, 37500-903, Itajubá, Minas Gerais, Brazil

matheus\_brendon@yahoo.com.br, guilhermefergom@gmail.com, sebas@unifei.edu.br,

lucasramonroque@gmail.com

<sup>2</sup>Physioterapy Department, Clinica Renove

91, Av. João Gonçalves da Costa, 37517-000, Maria da Fé, Minas Gerais, Brazil

brendaasfisio@gmail.com

**Abstract** Isogrid structure emerged in the early 1970s due the need for lightweight and high-performance model in the aeronautical industry, however, over the years, several other branches that also need these characteristics began to use this type of components. The present work aims to find the optimal design parameters for the lattice structure in order to minimize the Tsai-Wu failure index and the mass of the structure under compression loads by using two different metaheuristics algorithm: Genetic Algorithm (GA) and Sunflower Optimization (SFO). A Response Surface Methodology (RSM) was used for the purpose of setting up a series of experiments for adequate predictions of the responses and the generated models were used as objective functions for single and multi-objective optimizations. Finally, the results of both algorithms were compared with finite element method and the performance of the new meta-heuristics algorithm SFO was evaluated.

**Keywords:** Isogrid structure, Genetic Algorithm, Sunflower optimization, Response Surface Methodology, Finite Element Method.

## 1 Introduction

Optimization refers to the mathematical study of problems in which one seeks to minimize or maximize a function by modifying parameters within an experimental space [1]. The process is called mono-objective optimization when the desire is to optimize only one equation and multi-objective when it is desired to optimize several functions simultaneously.

The use of heuristic methods in optimization problems has grown in recent years due to the versatility of applications of these techniques, i.e., they are not linked to a specific model and can be applied to optimize any problem. Techniques such as genetic algorithm, particle swarm optimization and ant colony optimization are some of the techniques that are already established in the literature [2].

Other techniques have emerged in recent years, for example, Pereira *et al.* [3] introduced the Lichtenberg Algorithm which is based on the Lichtenberg figures. The author inspired in physical phenomena of radial intra-cloud lightning exploring the power of fractals making LA a hybrid algorithm, that is, composed of population and trajectory-based search methods. Gomes *et al.* [4] also developed an optimization algorithm recently called Sunflower optimization. This technique uses the sun as the best point and the others always look for it in the same way that a sunflower is always facing the sun.

The Sunflower optimization technique will be used in this work in conjunction with the already established genetic algorithm. Thus, for the development of the work, a Response Surface (RSM) Methodology was used for define which data, in what quantity and under what conditions should be collected during a given experiment, seeking, basically, to satisfy two major objectives : the highest possible statistical precision in the response and the lowest cost [5]. After initial analysis of the RSM, the finite element method was used for the structural calculations of the tube for each condition of the experiment generated by the model. With the results obtained, it

was possible to find the global equations that govern the problem.

This manuscript is organized as follows: Section 2, a general theoretical background about sunflower optimization and RSM is presented, Section 3 presents the methodological procedure. Section 4 presents the main results and discussions. Finally, Section 5 draws the conclusions.

## 2 Theoretical Background

### 2.1 Sunflower Algorithm Optimization

Gomes *et al.* [4] developed an optimization algorithm based on the phototropic movement of sunflowers. First, a pre-defined number of individuals are created and the aptitude of each one is calculated. The individual with the best aptitude value is called sun. To paraphrase the nature in which sunflowers are always pointed at the sun, individuals in the population will also always be looking for the best value of aptitude. In each iteration new individuals are generated, and they will also always look for the best point.

There are three variables in Sunflower Optimization: i) pollination rate ( $p_p$ ), ii) plant mortality rate ( $m_p$ ) and iii) survival rate of plants that will move in a controlled manner until the sun ( $p_s$ ). Individuals that are far from the optimum point can be removed from the algorithm and the variable that define it is the plant mortality rate. It can be thought that these individuals are sunflowers that are far from the sun and, because of this, do not receive energy and end up dying.

The pollination rate serves to create new individuals from those already exist in the population, that is, it is a percentage of the number of initial individuals that will reproduce. Individuals with the best aptitude value will reproduce with each other. It is simply assumed that each sunflower produces only one pollen gamete and reproduces itself individually.

Finally, some individuals will move towards the optimum point and the variable responsible for this is the survival rate of plants that will move in a controlled manner until the sun. The number of individuals that will move is random, following a normal distribution, between the individual's current position and the position of the sun. The Figure 1 shows a flowchart explain the algorithm.



Figure 1. SFO algorithm flowchart

## 2.2 Response Surface Methodology

The relationship between input and output in a process is often unknown. Response Surface Methodology is a technique for helping to find an equation that shapes the process in these situations [6]. In general, RSM can represent the relationship between process factors ( $w_1, w_2, w_3, \dots, w_n$ ) and the response variable ( $Y$ ) by equation 1.

$$Y = f(w_1, w_2, w_3, \dots, w_n) + \varepsilon \quad (1)$$

The response surface is made using an adjusted model and, when appropriate, its analysis will be approximately equivalent to the analysis of the actual surface. According to Montgomery [7], equation 2 represents the problems for RSM.

$$Y = \beta_0 + \sum_{i=1}^k \beta_i x_i + \sum_{i=1}^k \beta_{ii} x_i^2 + \sum_{i < j} \beta_{ij} x_i x_j + \varepsilon \quad (2)$$

$Y$  being the answer of interest,  $\beta$  the coefficients to be estimated,  $k$  the number of independent variables,  $x$  the parameters and  $\varepsilon$  the associated error term. The objective of RSM is to find the optimal process parameters so that the necessary conditions are met. The Central Composite Design (CCD) will be the arrangement used in this study as it is the arrangement most used to adjust second order models [7]. The CCD has a  $2^k$  factorial (blue),  $2k$  axial (green) and one central (red) points as shown in Figure 2a.

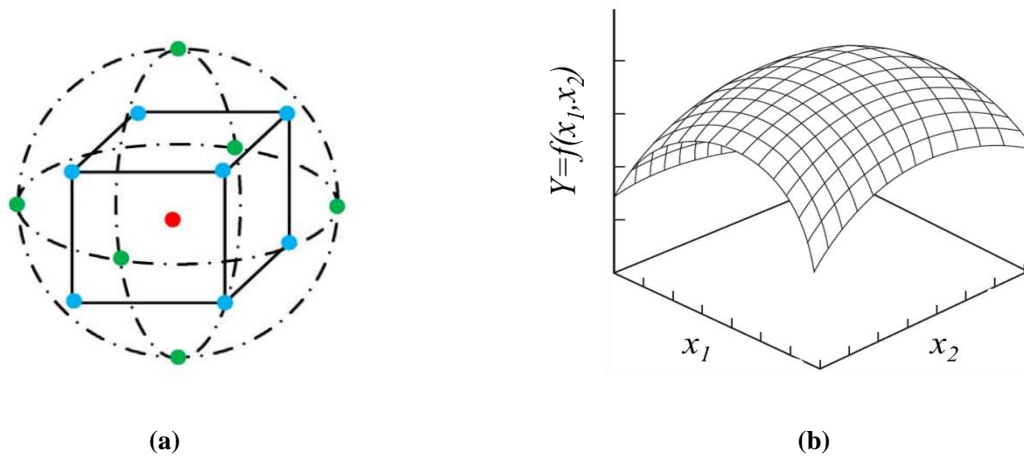


Figure 2. Typical response surface: (a) Central composite design [8] and (b) three-dimensional (adapted from Montgomery [7]).

## 3 Methodology

The objective functions used in this work are responses of an isogrid tube modeled in carbon fiber reinforced polymer composite (CFRP). The initial design of the tube can be done using 8 variables, namely: Angle of helical ribs with respect to the axial axis of the structure ( $\varphi$ ), width of circular ( $\delta_c$ ) and helical ( $\delta_h$ ) crosspieces, thickness ( $h$ ) of ribs, distance between circular ribs ( $\alpha_c$ ) and distance between helical ones ( $\alpha_h$ ), length ( $L$ ) and diameter ( $D$ ) of the tube.

The angle range between  $20^\circ$  and  $40^\circ$  was chosen based on the studies by Junqueira *et al.* [9] that evaluated three configurations of isogrid structures, modifying the angle between helical crossbeams, being  $26^\circ$ ,  $30^\circ$  and  $40^\circ$ . In addition, the same author used a fixed beam width equal to 4mm. The present study intends to vary this parameter between 2mm and 6mm to find the optimal set of the structure. The length ( $L$ ), diameter ( $D$ ) and thickness ( $h$ ) are constant and equal to 300mm, 30mm and 2.6mm, respectively.

The structure responses will be collected via numerical analysis using the finite element method. It was used an element with 8 nodes and six degrees of freedom, and the mesh size was 1.2mm. The two objectives of interest are: to minimize mass and to minimize the Tsai-Wu failure index of the structure under compression efforts. Thus, the CFRP T300/epoxy was used to construct the model and the properties shown in Table 2 were taken from the study of Madhavi [10], where the author made a characterization of the material used in the present study.

Table 2. Properties of CFRP T300/epoxy [10]

Propriety	Unit	Value	Standart
$E_1$	GPa	144	ASTM D3039
$E_2$	GPa	6.5	ASTM D3039
$G_{12}$	GPa	5.6	ASTM D3518
$S_{12}$	MPa	40	ASTM D3518
$\sigma_1^T$	MPa	1200	ASTM D3039
$\sigma_2^T$	MPa	17	ASTM D3039
$\sigma_1^C$	MPa	600	ASTM D3410
$\sigma_2^C$	MPa	80	ASTM D3410
ILSS	MPa	42	ASTM D2344
$\rho$	g/cm <sup>3</sup>	1.35	ASTM D3039
$\nu_{12}$	--	0.21	ASTM D3039

The boundary conditions used were based on a standard that deals with structural testing of lower-limb prostheses [11]. The structure was embedded in one end and a force of 4800 N was applied to the other as shown in Figure 3. It is important to note that the model was validated using experimental tests performed by Junqueira *et al* [9]. The design of experiments and the responses is shown in Table 3.

Table 3. Experimental matrix

$\varphi$ (°)	$\delta_c$ (mm)	$\delta_h$ (mm)	$TW_C$	Mass(g)
20	2	2	1.180	10.09
40	2	2	1.799	14.94
20	6	2	0.552	15.79
40	6	2	1.660	27.05
20	2	6	0.445	24.56
40	2	6	2.239	32.68
20	6	6	0.304	30.26
40	6	6	0.848	44.79
20	4	4	0.428	20.18
40	4	4	0.997	29.87
30	2	4	0.792	19.98
30	6	4	0.550	28.53
30	4	2	1.162	16.41
30	4	6	1.494	32.10
30	4	4	0.562	24.26
30	4	4	0.682	26.19
30	4	4	0.636	25.13
30	4	4	0.531	24.10
30	4	4	0.509	23.48
30	4	4	0.543	25.30

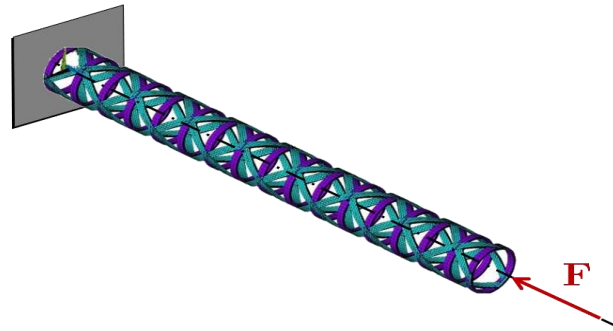


Figure 3 – Boundary condition for the model

After analyzing the response surface, one can find the objective functions that will be used for optimization: Table 4 shows the model for mass and for Tsai-Wu under compression efforts.

Table 4. Equations for mass and  $TW_c$ 

Response	$X_1$	$X_2$	$X_3$	$X_2^2$	$X_3^2$	$X_1X_2$	$X_1X_3$	$X_2X_3$	C
M	0.0003	0.339	3.052			0.05	0.03		-0.08
$TW_c$	0.031	-0.127	-1.142		0.136				2.536

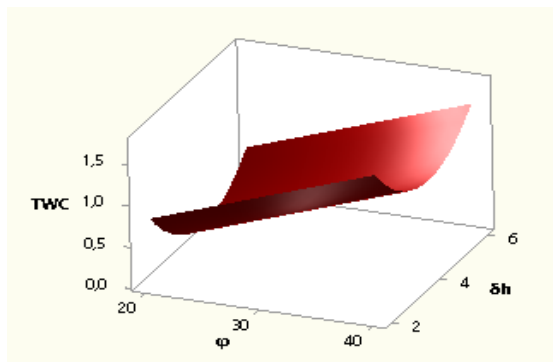
## 4 Results and Discussion

### 4.1 RSM analysis

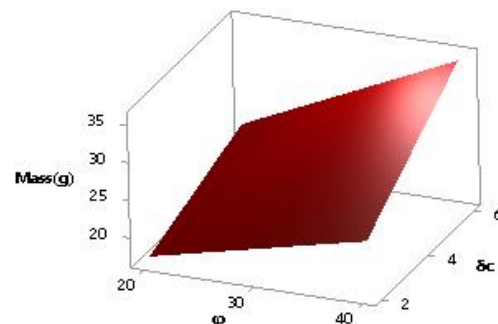
Table 5 shows the parameters of the model. Adjusted  $R^2$  shows how well the data fits the model, the higher, the better the data fit.  $S$  is measured in units of the response variable and represents the variation in the distance that the data values fall from the true response surface. The lower the  $S$  value, the better the model describes the response. Thus, the p-value less than 0,05 implies a significant model for the project. Finally, the Figure 4 shows the response surface for  $TW_c$  and mass model.

Table 5. Results of the model found for mass and  $TW_c$ 

Response	p-value	S	$R^2_{adj}$
Mass	0.000	0.68	99.19 %
$TW_c$	0.000	0.2	81.52 %



(a)



(b)

Figure 4. Response surface for (a)  $TW_c$  and (b) Mass.

The results in Table 5 show that the model is significant and well adjusted. Furthermore, figure 4 shows the response surface generated and gives us a sense of how the result varies with the design variables. For example, the response surface for mass suggests that smaller values of angle and circular width will be the optimum points of this problem.

### 4.2 Optimization

In this section, a single optimization was performed aiming at minimizing  $TW_c$  and minimizing mass with the restriction that  $TW_c$  was less than the unit 1. Thus, there is an optimization problem with restriction and another without restriction. Table 6 shows the results obtained with the optimization of responses. It is noticed that the results of both algorithms were the same, showing the reliability of using either one. However, the processing time of SFO is considerably longer than that of GA. In addition, a multi objective optimization was performed to minimize both  $TW_c$  and mass without any restriction. The results obtained are shown in Table 7 and Figure 5 shows the pareto boundary generated by both algorithms. Note that the results obtained by the two algorithms are the same, but GA has a shorter processing time.

Table 6. Optimization results from SFO and GA algorithm

	Mass		$TW_c$	
	SFO	GA	SFO	GA
Elapsed time (s)	19,45	1,45	13,54	0,17
Configuration	20 2,01 2,09	20 2,01 2,09	20 6 4,19	20 6 4,19
Results	10 ,26 g	10 ,26 g	0,2	0,2

Table 7. Multi objective optimization results from SFO and GA algorithm

	Multi objective optimization	
	SFO	GA
Elapsed time (s)	38,54	1,9
Configuration	20.6 5.59 4.82	20.6 5.59 4.82
Results - $TW_c$	0.12	0.12
Results - Mass	25.39	25.39

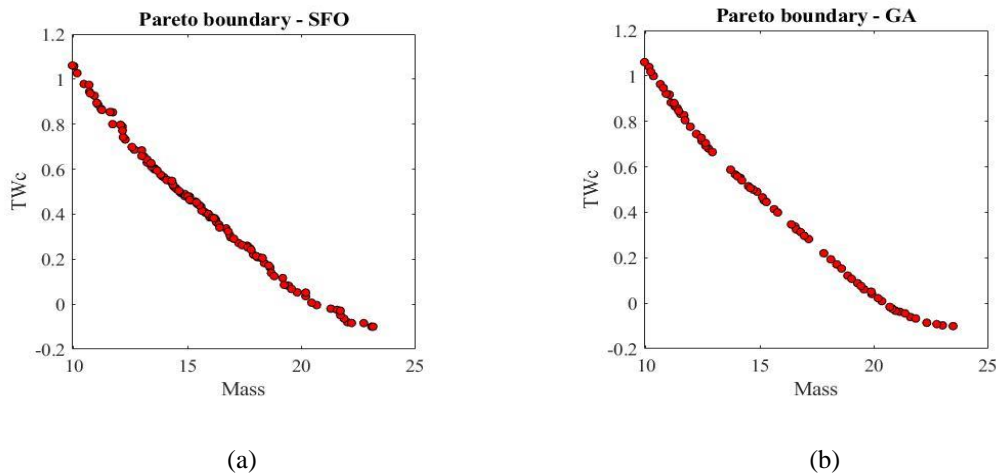


Figure 5. Pareto boundary for (a)  $TW_c$  and (b) Mass.

## 5 Conclusion

Both algorithms are reliable and have generated good results for the studied problem. SFO found the same points as the already established genetic algorithm (GA). The big drawback of SFO is its processing time, which is much longer than GA. For multi-objective optimization, SFO took 20x longer than GA.

The configuration found was simulated using the finite element methods and the results found were close to those found by the optimization, demonstrating the reliability of the proposed method.

**Acknowledgements.** The authors would like to acknowledge the financial support from the Brazilian agency CNPq (Conselho Nacional de Desenvolvimento Científico e Tecnológico), CAPES (Coordenação de Aperfeiçoamento de Pessoal de Nível Superior) and FAPEMIG (Fundação de Amparo à Pesquisa do Estado de Minas Gerais - APQ-00385-18).

**Authorship statement.** The authors hereby confirm that they are the sole liable persons responsible for the authorship of this work, and that all material that has been herein included as part of the present paper is either the property (and authorship) of the authors, or has the permission of the owners to be included here.

## References

- [1] Rao, Singiresu S. *Engineering optimization: theory and practice*. John Wiley & Sons, 2019.
- [2] Doerr, Benjamin. "Probabilistic tools for the analysis of randomized optimization heuristics." *Theory of Evolutionary Computation*. Springer, Cham, 2020. 1-87. [2]
- [3] Pereira, João Luiz Junho, et al. "Lichtenberg optimization algorithm applied to crack tip identification in thin plate-like structures." *Engineering Computations* (2020).
- [4] Gomes, Guilherme Ferreira, Sebastiao Simões da Cunha, and Antonio Carlos Ancelotti. "A sunflower optimization (SFO) algorithm applied to damage identification on laminated composite plates." *Engineering with Computers* 35.2 (2019): 619-626.
- [5] Kleijnen, Jack PC. "Response surface methodology for constrained simulation optimization: An overview." *Simulation Modelling Practice and Theory* 16.1 (2008): 50-64.
- [6] Khuri, Andr I. *Response surface methodology and related topics*. World scientific, 2006.
- [7] Montgomery, Douglas C. *Design and analysis of experiments*. John wiley & sons, 2017.
- [8] LIAN, B., Sun, T., & Song, Y. (2017). Parameter sensitivity analysis of a 5-DoF parallel manipulator. *Robotics and Computer-Integrated Manufacturing*, 46, 1-14.
- [9] Junqueira, Diego Morais, et al. "Design optimization and development of tubular isogrid composites tubes for lower limb prosthesis." *Applied Composite Materials* 26.1 (2019): 273-297.
- [10] M. MADHAVI. Design and analysis of filament wound composite pressure vessel with integrated-end domes. *Defence science journal*, 59(1):73-81, 2009.
- [11] NBR ISO 10328: 2002; Prosthetics - Structural testing of lower-limb prostheses Part 2: Test samples